Superresolution imaging of DNA tetrahedral nanostructures in cells by STED method with continuous wave lasers

Jiancong Du (杜建聪)[1], Suhui Deng (邓素辉)[2*], Shangguo Hou (侯尚国)[2], Lingling Qiao (乔玲玲)[3], Jianfang Chen (陈建芳)[3], Qing Huang (黄 庆)[2], Chunhai Fan (樊春海)[2], Ya Cheng (程 亚)[3], and Yun Zhao (赵 云)[1]**

[1]*College of Life Sciences, SiChuan University, Chengdu 610064, China*

[2]*Division of Physical Biology, and Bioimaging Center, Shanghai Synchrotron Radiation Facility, Shanghai Institute of Applied Physics, Chinese Academy of Sciences, Shanghai 201800, China*

[3]*Shanghai Institute of Optics and Fine Mechanics, Chinese Academy of Sciences, Shanghai 201800, China*

[*]*Corresponding author: dengsuhui@sinap.ac.cn;* [**]*corresponding author: zhaoyun@scu.edu.cn*

The first three authors contributed equally to this work

Received December 17, 2013; accepted January 15, 2014; posted online March 12, 2014

DNA tetrahedral nanostructures are considered to be new nanocarriers because they can be precisely controlled and hold excellent penetration ability to the cellular membrane. Although the DNA tetrahedral nanostructure is extensively studied in biology and medicine, its behavior in the cells with nanoscale resolution is not understood clearly. In this letter, we demonstrate superresolution fluorescence imaging of the distribution of DNA tetrahedral nanostructures in the cell with a simulated emission depletion (STED) microscope, which is built based on a conventional confocal microscope and can provide a resolution of 70 nm.

OCIS codes: 110.0180, 100.6640, 180.2520.
doi: 10.3788/COL201412.041101.

DNA nanostructures, emerged in early 1980s as a kind of nano-biomaterials, has been considered as the key materials due to its numerous functions and comprehensive applications[1]. DNA nanostructures have been proved to be permeable to the cellular membrane in the absence of transfection reagents[2,3]. Consequently, they can be used as a new type of nanocarrier to deliver the small-molecule into the cells. Compared with other nanocarriers like liposomes and inorganic nanostructures like gold nanoparticles[4], DNA nanostructures are purely biomolecules and can be precisely controlled because each ends of the chains can be designed to link certain functional molecules[5]. So far, a large amount of small-molecules like fluorescent dye, doxorubicin, nucleic acids and proteins[3,6,7] have been reported to be carried into the living cells.

As a typical nanostructure, three-dimensional (3D) tetrahedron can be self-assembled when the four single strands with partial complementary sequences are mixed in equimolar quantities buffer at 95° and cooled to 4°[8]. Several advantages of DNA tetrahedron promote us to explore optical imaging with such DNA structure. Firstly, DNA tetrahedron can enter live cells independently without transfection reagents and keep its initial structure without degradation for a long time[9]. Therefore, this type of DNA structure has the potential for live cell imaging. Secondly, the tetrahedron offers more modification sites to be coupled with target, drug or molecular beacon at one time, thus providing better biocompatibility and flexibility for various applications[10].

Typically, the DNA tetrahedral has a diameter of about 6 nm. Optical microscopy has failed in visualizing this structure due to the Abbe diffraction limit of ~200 nm[11]. Over the past decades, this limitation has driven research teams to develop several techniques to shatter the diffraction barrier and provide the resolution on the nanoscale[12−16]. Like stimulated emission depletion (STED) microscopy, a sub-diffraction fluorescent spot can be obtained by inhibiting the fluorescence at the periphery[17]. In this method, a doughnut-shaped depletion beam is used to be overlapped with a regular excitation spot and switch off the fluorescence of the surrounding phorophores through stimulated emission. In this way, a subdiffraction fluorescent spot is obtained in the center. On biological samples, this method has permitted visualization of individual syntaxin1 clusters in cells[18] and mitochondria in membranes with the resolution of 30−50 nm[19]. Moreover, the resolution down to

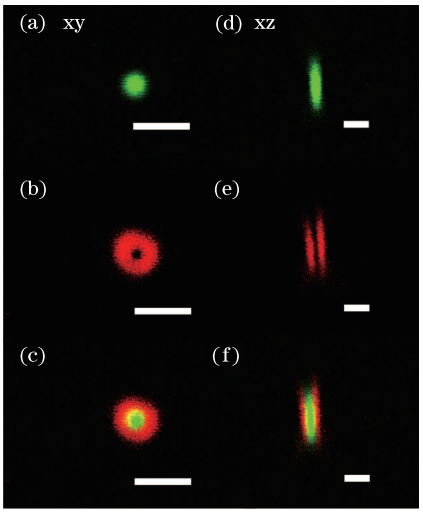

Fig. 1. (Color online) Focal intensity distributions of excitation (green) and STED (red) beams measured by imaging the 90-nm gold beads (a)−(c) on the focal plane and (d)−(f) along the axial dimension. Scale bar: 500 nm.

 © 2014 Chinese Optics Letters

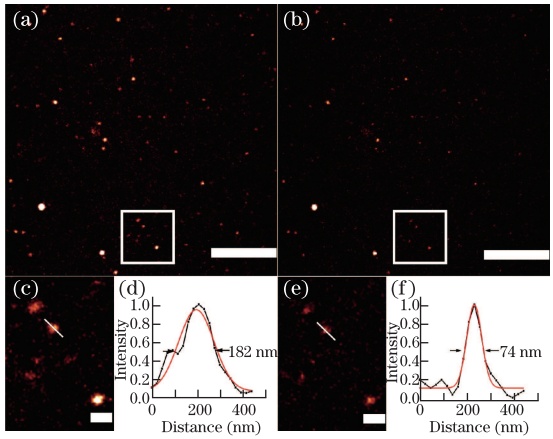

Fig. 2. (Color online) Comparison of (a) confocal and (b) STED images of 20 nm Yellow-green fluorescent particles mounted on a cover glass. (c) Confocal and (e) STED images in the white boxes in (a) and (b). (d) Confocal and (f) STED profiles of the bead indicated in (c) and (e) with a white line. Scale bars: 5 μm in (a) and (b), 500 nm in (c) and (e).

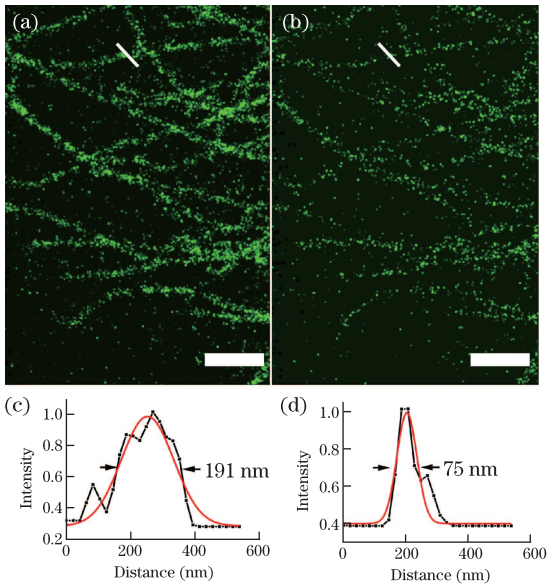

Fig. 3. (Color online) Comparison of (a) confocal and (b) STED images of the microtubule marked with Chromeo488. (c) Confocal and (d) STED profiles of the microtubule indicated in (a) and (b) with a white line. Scale bar: 2 μm.

several nanometers has been reported when imaging fluorescent nitrogen vacancies in diamond[20].

Although the setup of the STED microscopy is complex requiring that the excitation beam and the depletion beam should be reached to the sample synchronously in time and in space, STED instrumentation is compatible with most confocal scanning microscope and provide fast recording of the high resolution images. STED is the most direct methods to reduce the point spread function (PSF) and proved the sub-diffraction resolution without any mathematics. Since all the fluophores can undergo the stimulated emission, STED can work well with many dyes. In this letter, we aim to extend this method to DNA nanostructures in cellular-imaging applications. We show the distribution of DNA nanostructures in the cell with nanoscale precision.

In our experiments, the STED setup with continuous wave (CW-STED)[21] was built on an inverted microscope stand (Leica TCS SP5, Germany). The microscope setup was modified to provide access to the optical path of a depletion beam. A wavelength of 488 nm from an argon ion laser was employed for excitation and a CW beam at 592 nm for depletion was generated by a fiber-laser system (VFL-P-1500-592, MPB Communications, Canada). Both beams are expanded and recombined at a dichroic mirror before being delivered toward the objective lens. The fluorescence was collected by the same objective lens and separated from the laser beams with a bandpass filter (FF01-531/40-25, Semrock, USA) before being injected into a photomultiplier. By placing a quarter-waveplate and a vortex phase plate (VPP-A1, RPC photonics, USA) in the beam path, the depletion beam with a circular polarization was converted to be a focal doughnut when focused by the objective lens (OL) with numerical aperture of 1.4 (oil immersion, 63×). As shown in Fig. 1, the doughnut-shaped STED beam has formed when the PSF was measured by imaging of 90-nm gold nanoparticles. The excitation spot and the depletion beam spot were superposed well both on the focal plane and along the axial dimension.

To demonstrate the potential of this CW-STED microscope for nanoimaging, we firstly imaged 20-nm yellow-green fluorescent beads (Molecular Probes) on a cover slip and the microtubules of Hela cell. The nanospheres were mounted in medium Mowiol. The confocal and STED images are presented in Fig. 2. At the depletion power of 165 mW on the sample, the full width at half maximum (FWHM) of 74 nm was measured. With 10 different single nanoparticles, the resolution of the averaged STED profile was about 82 nm. In imaging, the pixel dwell time was 0.9 μs and the pixel size was 22 nm. Microtubules are a very useful system to determine the resolution of the imaging system. The microtubules filaments of Hela cell were immunofluorescently labelled with Chromeo 488 dye. Comparing confocal (Fig. 3(a))

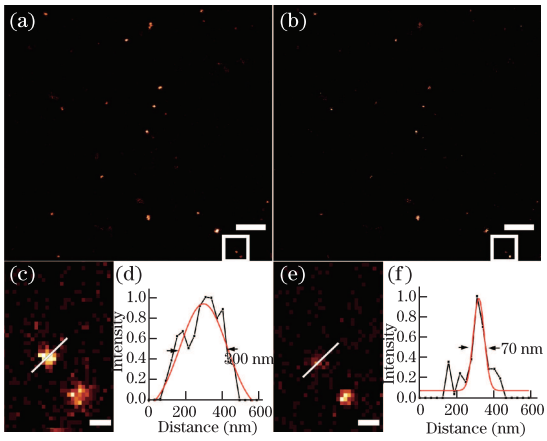

Fig. 4. (Color online) (a) Confocal and (b) CW-STED micrographs of tetrahedron marked by YoYo-1. (c) Confocal and (e) STED images in the white boxes in (a) and (b). (d) Confocal and (f) STED profiles of the bead indicated in (c) and (e) with a white line. Scale bars: 5 μm in (a) and (b), 500 nm in (c) and (e).

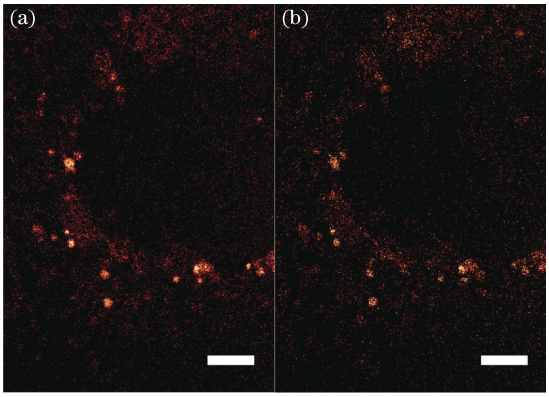

Fig. 5. (Color online) The distribution of DNA tetrahedral nanostructure in Hela cells imaged with (a) Confocal and (b) CW-STED microscope. Pixel size: 30 nm. Scale bar: 5 μm.

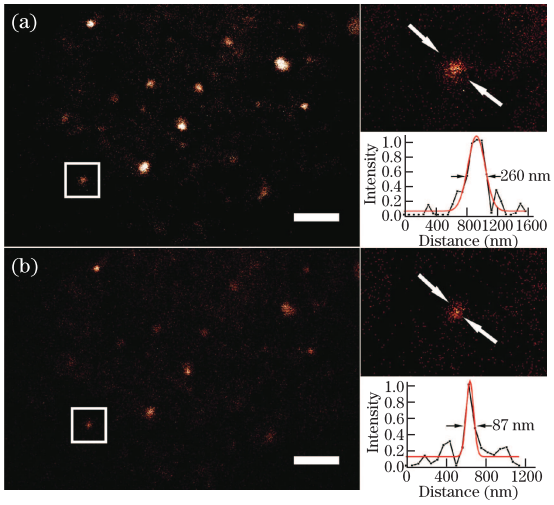

Fig. 6. (Color online) Comparison of confocal and STED images of tetrahedron in Hela cells. (a) Confocal and (b) CW-STED micrographs of tetrahedron marked by Alexa488. Magnified view of the raw data in the boxed areas are shown in right. Pixel size: 24 nm. Scale bar: 5 μm.

with STED (Fig. 3(b)) images of tubulin filaments, the resolution is obviously improved by CW-STED method at an average CW-STED power of 149 mW on the sample, line profile of the fluorescence intensity along the white line in Fig. 3(d) was measured as small as 75 nm in the CW-STED image.

Next, to evaluate the power of the STED nanoscopy on imaging the DNA nanostructures, we imaged the DNA nanostructures dispersed on the coverslip. To visualize its spatial distribution, we labeled the DNA nanostructures with $C_{49}H_{58}I_4N_6O_2$ (YOYO-1) by mixing 50-nmol/L tetrahedron with 1.28 μmol/L YOYO-1 for an hour. Comparison shows that many small clusters of DNA nanostructures are discernible in the STED image but not in the corresponding confocal image (Fig. 4). Figure 4(b) displays that large clusters of the DNA nanostructures are formed. The STED data shows that the distribution of the cluster size of DNA nanostructures is in the range of 70−400 nm due to the different degree of the aggregation. The FWHM value measured in the STED mode indicates that a resolution down to 70 nm is achieved by this system, which means that by using STED at 165 mW on the sample, we obtain a four-fold improvement in resolution over standard confocal microscopy.

Finally, the CW-STED nanoscopy was employed to image the distribution of DNA nanostructures in a fixed Hela cell. Before imaging, Hela cells on the coverslip were maintained in Dulbecco's minimum essential medium (DMEM, Gibco) which contains 10% fetal bovine serum (FBS, Gibco) and the 100 nM tetrahedron for 6 hours. Then the cells were fixed with paraformaldehyde for 20 min at room temperature. For fluorescence imaging, we labeled DNA nanostructures with Alexa 488 dye at 3' end of DNA chain of the tetrahedron. The results indicate that DNA nanostructures also form clusters and are mainly distributed on the cytoplasm (Fig. 5), which was displayed much clearly in the STED than in the corresponding confocal image. The details of the distribution are displayed in the Fig. 6, where the data shows that most tetrahedrons are distributed in the size ranging from 87 to 230 nm in the cell. The resolution is enhanced from 260 nm in confocal mode to 87 nm in STED microscope, corresponding to a threefold improvement. The focal power of the CW-STED beam was 181 mW on the sample.

In conclusion, we build a CW-STED microscope and prove the power of this STED nanoscopy on imaging the DNA nanostructures in cell. The results show that three- to four-fold improvement in resolution of our home-built STED setup over standard confocal microscope is obtained. The resolution is proved to be about 70 nm. The data shows that the DNA tetrahedron forms clusters in periphery of the nucleus and the the distribution of the cluster size of DNA nanostructures is in the range of 87−230 nm in cells due to the different degree of the aggregation.

This work was supported by the National Natural Science Foundation of China under Grand Nos. 61008056, 21227804, 61078016, and 61378062).

References

1. A. V. Pinheiro, D. Han, W. M. Shih, and H. Yan, Nature Nano. **6,** 763 (2011).
2. S. Ko, H. Liu, Y. Chen, and C. Mao, Biomacromolecules **9,** 3039 (2008).
3. A. S. Walsh, H. Yin, C. M. Erben, M. J. A. Wood, and A. J. Turberfield, ACS Nano **5,** 5427 (2011).
4. W. T. Al-Jamal and K. Kostarelos, Acc. Chem. Res. **44,** 1094 (2011).
5. S. Modi, M. G. Swetha, D. Goswami, G. D. Gupta, S. Mayor, and Y. Krishnan, Nature Nano. **4,** 325 (2009).
6. D. A. Giljohann, D. S. Seferos, A. E. Prigodich, P. C. Patel, and C. A. Mirkin, J. Am. Chem. Soc. **131,** 2072 (2009).
7. I. Heller, G. Sitters, O. D. Broekmans, G. Farge, C. Menges, W. Wende, S. W. Hell, E. J. G. Peterman, and G. J. L. Wuite, Nature Methods **10,** 910 (2013).
8. R. P. Goodman, I. A. T. Schaap, C. F. Tardin, C. M. Erben, R. M. Berry, C. F. Schmidt, and A. J. Turberfield, Science **310,** 1661 (2005).

9. J. Li, H. Pei, B. Zhu, L. Liang, M. Wei, Y. He, N. Chen, D. Li, Q. Huang, and C. Fan, ACS Nano **5,** 8783 (2011).
10. J.-W. Keum and H. Bermudez, Chem. Commun. 7036 (2009).
11. E. Abbe, Archiv für mikroskopische Anatomie **9,** 413 (1873).
12. S. W. Hell, Science **316,** 1153 (2007).
13. S. Deng, J. Chen, Q. Huang, C. Fan, and Y. Cheng, Opt. Lett. **35,** 3862 (2010).
14. B. Huang, H. Babcock, and X. Zhuang, Cell **143,** 1047 (2010).
15. Y. Chen, H. Guo, W. Gong, L. Qin, H. Aleyasin, R. R. Ratan, S. Cho, J. Chen, and S. Xie, Chin. Opt. Lett. **11,** 011703 (2013).
16. L. Li, Y. Ebihara, R. Shirogane, and M. Saito, Chin. Opt. Lett. **10,** S21003 (2012).
17. S. W. Hell and J. Wichmann, Opt. Lett. **19,** 780 (1994).
18. J. J. Sieber, K. I. Willig, R. Heintzmann, S. W. Hell, and T. Lang, Biophys. J. **90,** 2843 (2006).
19. D. C. Jans, C. A. Wurm, D. Riedel, D. Wenzel, F. Stagge, M. Deckers, P. Rehling, and S. Jakobs, Proc. Natl. Acad. Sci. Unit. States Am. **110,** 8936 (2013).
20. E. Rittweger, K. Y. Han, S. E. Irvine, C. Eggeling, and S. W. Hell, Nature Photon. **3,** 144 (2009).
21. G. Moneron, R. Medda, B. Hein, A. Giske, V. Westphal, and S. W. Hell, Opt. Express **18,** 1302 (2010).